Cellular and Molecular Life Sciences (2026) 83:385
https://doi.org/10.1007/s00018-026-06361-4

ORIGINAL ARTICLE

Meprin β is specifically inhibited by its cognate synthetic propeptide

Fred Armbrust[1] · Hannah Bruhn[1] · Kira Bickenbach[1] · Nicolas Steen[1] · Sapir Shcoory[2] · Nikolaos Afratis[3] · Nele Korn[1] · Hagen Körschgen[4] · Catherine Moali[5] · Claus U. Pietrzik[6] · Irit Sagi[2] · Christoph Becker-Pauly[1]

Received: 9 April 2026 / Revised: 23 June 2026 / Accepted: 16 July 2026
© The Author(s) 2026

Abstract

Meprin β is a zinc-dependent metalloprotease of the astacin family highly expressed in kidney and intestine. Dysregulation of meprin β expression and activity was observed in several pathological conditions such as Alzheimer's disease, cancer, fibrosis, and inflammatory bowel disease. Therefore, inhibition of meprin β could be a promising therapeutic option to treat pathological conditions influenced by this protease. However, available small-molecule compounds such as the broad-spectrum metalloproteinases inhibitors marimastat or actinonin lack specificity. Hence, more selective meprin β inhibitors needs to be developed. Here, we provide evidence that the synthetically generated cognate meprin β propeptide serves as highly specific inhibitor for the protease (IC_{50} = 1.35 µM), while other related metalloproteases such as meprin α and a disintegrin and metalloproteinases (ADAMs) are not affected. Employing a targeted approach revealed that removal of the last four C-terminal amino acids of the propeptide significantly improved its inhibitory capacity (IC_{50} = 0.68 µM). In cell-based experiments, treatment with the propeptide resulted in diminished meprin β activity and decreased cleavage of its substrates, including the interleukin-6 receptor (IL-6R) and the G protein-coupled receptor latrophilin-3 (LPHN3). Suitability was further confirmed in ex vivo cultivated organotypic brain slices, where the administration of the propeptide also resulted in decreased meprin β activity and diminished latrophilin-3 cleavage. Thus, not only the synthetic wildtype propeptide but especially a C-terminally truncated propeptide of meprin β represent highly specific inhibitors with potential for therapeutic application.

Keywords Protease · Metalloprotease · Inhibitor · IL-6R · Latrophilin-3 · Amyloid precursor protein · Inflammation · Alzheimer's disease

Fred Armbrust, Hannah Bruhn and Kira Bickenbach contributed equally to this work.

✉ Irit Sagi
irit.sagi@weizmann.ac.il

✉ Christoph Becker-Pauly
cbeckerpauly@biochem.uni-kiel.de

[1] Biochemical Institute, Unit for Degradomics of the Protease Web, Kiel University, Otto-Hahn-Platz 9, Kiel 24118, Germany

[2] Dept. of Immunology and Regenerative Biology, Weizmann Institute of Science, Max and Lillian Candiotty Building, Room 207, 234 Herzl St. Rehovot, Rehovot 76100, Israel

[3] Department of Agricultural Development, Agri-food & Management of Natural Resources, National and Kapodistrian University of Athens, Evripos Campus, Psachna, Evia 34400, Greece

[4] Institute of Pathobiochemistry, University Medical Center Mainz, Mainz, Germany

[5] Tissue Biology and Therapeutic Engineering Laboratory (LBTI-UMR 5305 CNRS), Lyon University, Lyon, France

[6] Molecular Neurodegeneration, Institute of Pathobiochemistry, University Medical Center Mainz, Mainz, Germany

Published online: 23 July 2026

Background

Meprin β, a zinc-dependent metalloprotease of the astacin family, is highly expressed in the kidney and intestine [1]. While its physiological role in the kidney has not been fully addressed yet, meprin β has been shown to play a crucial role for the host-microbiome homeostasis in the intestine by cleaving mucin-2, a key component of the mucus layer, and the bacterial agglutination factor galectin-3 [2, 3]. Thus, dysregulation of meprin β in the gut is associated with bacterial overgrowth and chronic intestinal inflammation [4]. Moreover, meprin β is tissue-specifically upregulated in different pathological conditions such as fibrosis [5] or Alzheimer's Disease (AD) [6, 7], where it cleaves procollagens and the amyloid precursor protein (APP), respectively. Increased meprin β activity additionally contributes to inflammatory processes by releasing the soluble interleukin-6 receptor (IL-6R) through ectodomain shedding and thereby inducing pro-inflammatory IL-6 trans-signaling [8]. Given its involvement in these pathological conditions, targeting meprin β could be a promising therapeutic approach. However, developing applicable and selective inhibitors has proven challenging. On the one hand, hydroxamate-based metalloproteinase inhibitors such as batimastat or actinonin can be used to inhibit meprin β activity [9]. However, their use as therapeutic meprin β inhibitors would presumably come along with detrimental side effects resulting from their lack of specificity [10, 11]. On the other hand, mammalian plasma fetuin-B was identified as potent endogenous meprin β inhibitor. However, its therapeutic potential is limited by its relatively large size of 40 kDa and the inhibition of other proteases of the astacin family [12]. A more promising approach involved the development of a transition-state analog inhibitor (named F2) featuring an acidic amino-acid moiety surrounding a non-cleavable phosphinic group, which demonstrated good affinity for inhibiting meprin β [13]. However, the synthesis of this compound is challenging and both time- and cost-intensive.

The aim of this study was to investigate whether the synthetically produced cognate propeptide of meprin β has sufficient specificity and bioavailability and is therefore suitable as a potential therapeutic drug. A similar approach has been successfully conducted with the metalloproteases ADAM10 and ADAM17. It has been shown that the addition of their recombinantly expressed prodomains lead to the inhibition of protease activity [14, 15]. Interestingly, in a tumor mouse model, the intravenous injection of the recombinant prodomain of ADAM17 markedly reduced tumor burden in the lung, and partially in liver and kidney [16].

Methods

Recombinant enzymes and inhibitors

Recombinant meprins were obtained as described before [17]. Bone morphogenetic protein 1 (BMP1) was produced in HEK293-EBNA cells as described in [18]. Fetuin-B was purified as described before [19]. Actinonin (A6671) was purchased from Sigma Aldrich. Propeptide variants (Table 1) were generated by Genosphere BT. For the experiment comparing the inhibition of wildtype (WT) meprin β and meprin β R238Q, both meprin variants were immunoprecipitated with flag tag antibody (20543-1-AP, proteintech) and Protein G Dynabeads (Thermo Fisher Scientific) from the lysate of transfected HEK cells. For a detailed protocol see [13].

Microscale thermophoresis

Microscale thermophoresis (MST) was used as a fluorescent-based method to evaluate protein-ligand interactions [20]. MST works as follows: A fluorescent-labeled protein is incubated with different concentrations of a potential ligand and fluorescence intensity, measured in arbitrary units, is detected over time while a temperature gradient is applied, impacting the migration of the fluorescent-labeled protein, which depends on ligand binding. The ratio F_{hot}/F_{cold} yields the normalized fluorescence, F_{norm}, which is plotted against the logarithmic concentrations of the ligand. Pro- and mature meprin β were labeled with NT-647 according to the manufacturer's instructions. The labeled meprin β (30 nM) was incubated with different concentrations of the synthetically produced propeptides ranging from 6 pM to 50 µM. Subsequently, mixtures were transferred to capillaries and measured using the Monolith NT.115 device (NanoTemper Technologies GmbH). The dissociation constant (K_D) was calculated using the NanoTemper software.

Table 1 Sequences of meprin β propeptide variants

Name	Sequence
propeptide	TPENFDVDGGMDQDIFDINEGLGLD-LFEGDIRLDRAQIR
propeptideΔN	QDIFDINEGLGLDLFEGDIRLDRAQIR
propeptideΔC	TPENFDVDGGMDQDIFDINEGLGLD-LFEGDIRLDR
propeptideΔN/C	QDIFDINEGLGLDLFEGDIRLDR
propeptideΔC D36A	TPENFDVDGGMDQAIFDINEGLGLD-LFEGDIRLDR

Cell culture, transfection and lysis

HEK293T cells and HEK293T cells deficient for ADAM10 and ADAM17 (HEK293T_A10/17$^{-/-}$) [21] were maintained at 37 °C in an atmosphere of 5% CO_2 in Dulbecco´s modified Eagles´s medium (DMEM; Thermo Fisher Scientific) supplemented with 10% fetal bovine serum (FBS; Thermo Fisher Scientific). Transfection with plasmid DNA, pre-mixed with polyethyleneimine (PEI) (1:3) in serum-free medium was performed at 80–90% cell confluence. Plasmid DNA containing cDNA for human soluble ADAM10 ectodomain, mouse ADAM10, human BMP1, N-terminal HA-tagged mouse latrophilin (latrophilin-3), human meprin α, human meprin β wt, human meprin β R238Q, human IL-6R, human APP695 and pcDNA3.1 as empty vector control in different combinations were added together with transfection reagent to the cell culture medium. After 24 h, the cell medium was changed to serum-free DMEM. For cell surface activity measurements, after another 24 h cells were washed with phosphate-buffered saline (PBS) and counted using a Neubauer counting chamber. If indicated, the propeptide or its C-terminally truncated variant (propeptideΔC) was added at the specified concentrations concurrently with serum removal. After an initial incubation period of 3 h, the same concentration of the propeptide variant was added again for an additional 3 h. The cells were harvested, washed with PBS and then incubated in lysis buffer (1% (v/v) Triton X-100 in PBS (pH 7,4) with cOmplete™ protease inhibitor cocktail (Roche), 1% (v/v) Triton X-100 in PBS (pH 7,4)) for 30 min at 4 °C. Lysates were centrifuged at 15,000 x g at 4 °C, cell debris was discarded. The protein concentration in the lysates was determined using the BCA assay kit (Thermo Fisher Scientific) according to manufacturer's instructions.

SDS-PAGE and western blot analysis

Cell lysates or supernatants were incubated for 10 min at 95 °C with sample buffer (50 mM Tris-HCl (pH 6.8), 2% (w/v) sodium dodecyl sulphate (SDS), 0.1% bromophenol blue (Merck), 10% (v/v) glycerol, 100 mM dithiothreitol (DTT)). The protein separation was performed by SDS-PAGE (120 V, 90 min) using the Mini-PROTEAN® system (Bio-Rad). Western blot was accomplished with a tank-blot system (Bio-Rad) onto PVDF membranes (0.8 A, 2 h, 4 °C). Afterwards, the membranes were blocked with 5% milk (w/v) in TBS for 1 h at room temperature. The primary antibodies against glyceraldehyde 3-phosphate dehydrogenase (GAPDH) (14C10, Cell Signaling, dilution 1: 5,000), HA-tag (C29F4, Cell Signaling), meprin β (polyclonal antibody, generated against a peptide from the meprin/A5 protein/receptor protein tyrosine phosphatase μ (MAM) domain (Pineda)), latrophilin-3 (B-6, Santa Cruz), IL-6R (4–11, kindly provided by Stefan Rose-John (Kiel, Germany)), APP/sAPPα (6E10, Thermo Fisher), sAPPβ + Asp (Pineda, [22]) unless not stated differently in the respective figure legend, were incubated using a dilution of 1:1,000 with the membrane over night at 4 °C. Horseradish peroxidase-conjugated secondary antibodies (Jackson ImmunoResearch) were diluted in TBS-T (TBS with 0.1% (v/v) Tween® 20) and incubated with the membranes for 1 h at room temperature. The chemiluminescence signal was detected in the Intelligent Dark Box (Fujifilm) or Amersham ImageQuant™ 800 (Cytiva) using the Super Signal® West Pico/Femto Kits (Thermo Fisher Scientific) according to manufacturer's instructions. Western blot signals were quantified with ImageJ.

Fluorogenic peptide-based activity assay

The activity of recombinant proteases, proteases on the cell surface and proteases in conditioned supernatants were measured with well-established quenched fluorogenic peptide substrates summarized in Table 2.

For this purpose, 5 nM of recombinant enzymes, 500,000 cells or up to 90 µl conditioned supernatant was transferred in 96-well plates in a total volume of 100 µl PBS or DMEM only. For the measurement of meprin α and meprin β in conditioned medium, the enzymes were proteolytically activated with 5 µg/ml trypsin (Sigma Aldrich) and trypsin was afterwards inhibited by ovomucoid (Sigma Aldrich) both steps for 10 min at 37 °C. For activity measurement of human angiotensin converting enzyme (ACE1, Sigma-Aldrich) 50 mM HEPES, 300 mM NaCl (pH 8.0), for human ACE 2 (Sigma-Aldrich) 50 mM Tris, 150 mM NaCl (pH 7.5) and for MMP1/2/14 (R&D) 50 mM HEPES, 10 mM $CaCl_2$ (pH 7.5) were used as buffer. Murine ovastacin was heterologously expressed and purified as previously described [30]. Activation was achieved with human plasmin (Haematologic Technologies). Enzyme kinetic measurements were performed as described [29]. If indicated in the figure, additional inhibitors, meprin β propeptide variants, fetuin-B, or actinonin, were added and preincubated for 10 min at 37 °C. Afterwards, the respective peptide substrate was added as depicted in Table 2. The measurement was conducted at 37 °C for 1–2 h. Every 30 to 60 s, the fluorescence at the wavelengths indicated in Table 2 was monitored. Relative fluorescent units (RFUs) were normalized to the

Table 2 Peptide substrates. The final concentration in the assays is indicated in the $c_{substrate}$ column. The references column summarizes successful use of the particular fluorogenic peptides to show peptidase activity of the respective protease. ADAM10 substrate was obtained from BioZyme Inc., MMP1/2/14 substrate from R&D Systems and ACE1/ACE2/ADAM17 substrates from Sigma Aldrich, ovastacin substrate from Biosyntan and the others from Genosphere BT. 5-fam: 5-carboxyfluorescein, dabcyl: Acetyl-dArg(3)-dGlu(3)-hexaminoyl-K-4-((4-(Dimethylamino)phenyl)azo)benzoic, mca: 7-methyloxycoumarin-4-yl, dnp: K-ε-dinitrophenyl

Substrate for	Sequence	$^{\lambda}$exitation	$^{\lambda}$emission	^{c}substrate	References
ADAM10	(dabcyl)-PRYEYK-MGK-(5-fam)	480 nm	530 nm	10 µM	[23]
BMP1	(mca)-YVADAPK-(dnp)	320 nm	405 nm	20 µM	[24]
Meprin α	(mca)-HVANDPIW-(dnp)	320 nm	405 nm	20 µM	[3]
Meprin β	(mca)-EDEDED-(dnp)	320 nm	405 nm	25 µM	[1]
Meprin β R238Q	(mca)-EDAEDA-(dnp)	320 nm	405 nm	25 µM	[13]
MMP1, MMP2, MMP14	(mca)-PLGL-(dpa)-AR-NH_2	320 nm	405 nm	20 µM	[25]
ACE1	(mca)-RPPGFSAFK-(dnp)	320 nm	405 nm	10 µM	[26]
ACE2	(mca)-APK(Dnp)-OH	320 nm	405 nm	10 µM	[27]
ADAM17	(abz)-LAQA-VRSSSR-(dpa)	320 nm	405 nm	10 µM	[28]
Ovastacin	Ac-RE(Edans)-DR-Nle-VGDDPYK(Dabcyl)-NH_2	350 nm	520 nm	25 µM	[29]

respective control samples only containing the respective background medium and peptide substrate. Negative values were set to 0. The bar graphs display the slope of the linear gain of fluorescence within the linear range (max. first 30 min). K_i (inhibition constant) values were determined using GraphPad Prism.

Preincubation and stability testing of propeptide inhibitor

To analyse stability properties of propeptideΔC preincubations at a concentration of 20 µM at different temperatures for 20 min, freeze-thrawn for indicated times or preincubated using PBS with different pH values for 20 min (buffer only as a control, measurement of meprin β activity after adjustment to pH 7.4). To test proteolytic stability propeptideΔC (20 µM) was incubated with trypsin (1–5 µg/ml) in PBS, chymotrypsin (EDQM) (1–5 µg/ml) in 100 mM Tris, 10 mM $CaCl_2$ (pH 7.8) or thrombin (Sigma) (1–5 µg/ml) in PBS for 20 min at 37 °C or in case of chymotrypsin at 30 °C. To inhibit trypsin/chymotrypsin afterwards PMSF (phenylmethylsulfonyl fluoride) (final 1 mM) was added. To test stability in mouse serum, mouse serum from C57BL/6 mice were incubated in a 1:1 ratio at 37 °C with 200 µM propeptideΔC for 20 min. Corresponding incubation conditions without propeptideΔC were used as controls for subsequent activity assays.

Experimental animals and Generation, cultivation and lysis of organotypic brain slice cultures (OBSCs)

Mice were maintained under constant environmental conditions (12-hour light-dark cycles, temperature) and in an individually ventilated cage system with food and drinking water ad libitum in accordance with the ethical standards and current guidelines of the European Union. The animals were kept solely for organ removal. This is not an animal experiment in the sense of the German Animal Welfare Act, as no animal was stressed or manipulated. Therefore, no further approval from the responsible authority (Ministry of Agriculture, Rural Areas, Europe and Consumer Protection including the Ethics Committee according to Sect. 15 of the Animal Welfare Act) was required. Meprin β knock-in mice overexpressing meprin β with C-terminal HA tag in astrocytes were generated [22]. Rosa26$^{Mep1b-HA}$ mice, which were heterozygous for GFAP-dependent Cre, are termed as GFAP$^{Cre+/-}$;Rosa26$^{Mep1b-HA}$ mice (or briefly Cre$^{+/-}$). The respective Cre-negative control animals are referred to as GFAP$^{Cre-/-}$;Rosa26$^{Mep1b-HA}$ (or briefly Cre$^{-/-}$). Mice were sacrificed by cervical dislocation and brains were isolated. OBSC generation, cultivation and lysis was conducted as described in [22]. Half of the brain slices of each genotype were randomly selected and treated with 5 µM propeptideΔC together with the serum-free medium 24 h prior harvesting, while the rest were left untreated. Additional 5 µM propeptide were added every 6 h.

Statistical analysis and illustrations

All statistical analyses were performed with the GraphPad Prism 10 software. Conducted tests are stated in the respective figure descriptions (*: $p<0.05$; **: $p<0.01$; ***: $p<0.001$). Protein structures were generated using Chimera 1.17.3. The figures were created with Microsoft PowerPoint and BioRender.com.

Results

Meprin β is inhibited by exogenous addition of its propeptide

To analyze whether the propeptide of meprin β serves as a specific inhibitor, we synthesized the propeptide based on the amino acid sequence annotated in uniprot (Fig. 1A). From AlphaFold modeling, the complex of active meprin β together with the synthetic cognate propeptide clearly resembles the structure of pro-meprin β, where the propeptide is covalently linked to the enzyme with only little differences in the very C-terminal part of the propeptide. MST measurements were conducted to analyze the interaction between recombinant meprin β and the synthetically produced propeptide and the sigmoidal curve obtained validated an interaction with a K_D of 3.95 µM (Fig. 1B and Supplementary Figure S1A). As negative control, the propeptide was additionally applied to pro-meprin β, which showed no interaction as indicated by the absence of a sigmoidal curve (Supplementary Figure S1B).

To evaluate the inhibitory potential of the propeptide, we added various concentrations to recombinant meprin β in a fluorescent-based peptide cleavage assay (Fig. 1C). In the micromolar range, we observed a concentration-dependent decrease in activity, up to 90% inhibition with 10 µM propeptide. We also analyzed the known meprin β inhibitors actinonin and fetuin-B in the same experimental setup and estimated IC_{50} values of about 7.5 µM for actinonin and 200 nM for fetuin-B (Fig. 1D and E), which is in the range of previous observations [9, 12, 31]. To investigate the inhibitory capacity of the propeptide towards proteolytically shed meprin β, we analyzed soluble meprin β from conditioned HEK cell supernatants (Fig. 1F). Therefore, we transfected HEK ADAM10/17$^{-/-}$ cells with meprin β and ADAM10. Of note, ADAM10 and ADAM17 are sheddases of meprin β releasing the ectodomain of meprin β to the supernatant, which was also the case upon retransfection of ADAM10. Of note, in the conditioned medium meprin β activity was completely abolished by addition of the propeptide in a concentration-dependent manner. To assess inhibition of meprin β upon application of the propeptide, actinonin and fetuin-B to the conditioned medium, we determined the necessary concentrations for each individual inhibitor leading to a similar reduction of meprin β activity of approximately 75% (Fig. 1G).

Regarding pathological conditions, the inhibition of increased meprin β activity, especially in the membrane-bound state, is important. Therefore, we quantified meprin β cell surface activity using transfected HEK cells (Fig. 1H). We observed that membrane-bound meprin β was concentration-dependently inhibited by its propeptide, down to 10% remaining activity at a concentration of 10 µM propeptide. To further investigate the inhibition of membrane bound meprin β by the propeptide, actinonin, and fetuin-B, we applied these inhibitors at concentrations previously established in Fig. 1G (Fig. 1I). Notably, the propeptide resulted in meprin β activity inhibition of 80%, while actinonin and fetuin-B revealed only inhibition of about 40%. In terms of inhibiting the membrane-bound form of meprin β, these results indicate that the inhibitory potency of the propeptide exceeds that of actinonin and fetuin-B. Additionally, we examined the effects of meprin β inhibition using HEK ADAM10/17$^{-/-}$ cells and observed similar results (Supplementary Figure S2A, B).

The inhibition of meprin β by its synthetic propeptide is highly specific

To assess the specificity of the meprin β propeptide as an inhibitor, we additionally tested other related proteases. Therefore, we examined meprin β's closest relative meprin α, BMP1 - another member of the astacin protease family group, and ADAM10, which share a similar substrate pool with meprin β. Peptide cleavage assays revealed that the propeptide of meprin β is not capable of inhibiting recombinant meprin α (Fig. 2A). This finding was further confirmed with HEK cell-derived meprin α, which, however, could be inhibited by actinonin and fetuin-B (Fig. 2B). Additionally, recombinant BMP1 (Fig. 2C) and ADAM10 (Fig. 2D) were not inhibited by the propeptide, demonstrating the remarkable specificity of the meprin β propeptide as an inhibitor.

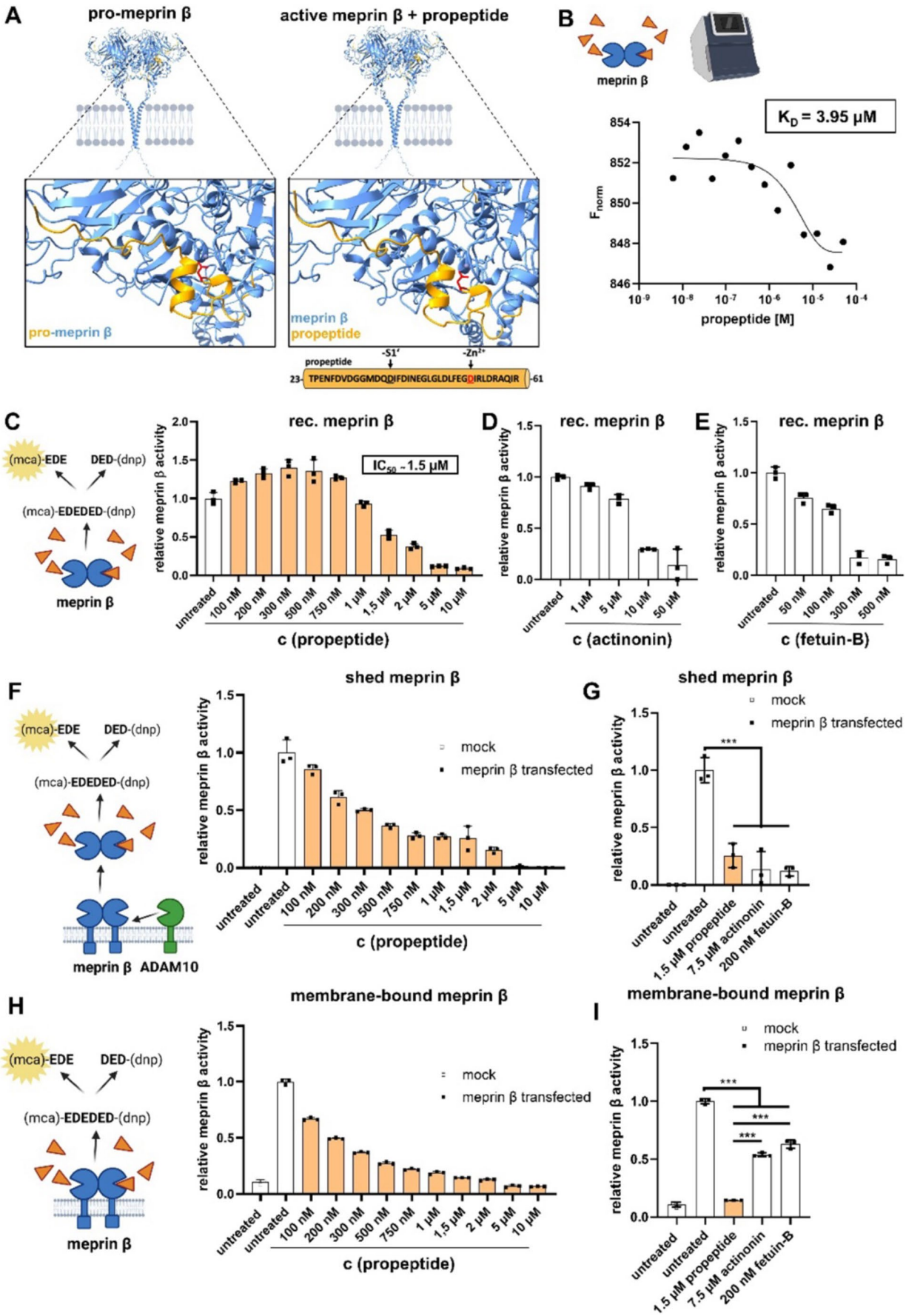
A
pro-meprin β
active meprin β + propeptide
pro-meprin β
meprin β
propeptide
propeptide
-S1'
-Zn2+
23- TPENFDVDGGMDQDIFDINEGLGLDLFEGDIRLDRAQIR -61
B
meprin β
KD = 3.95 µM
Fnorm
propeptide [M]
C
(mca)-EDE
DED-(dnp)
(mca)-EDEDED-(dnp)
meprin β
rec. meprin β
relative meprin β activity
IC50 ~1.5 µM
untreated
100 nM
200 nM
300 nM
500 nM
750 nM
1 µM
1,5 µM
2 µM
5 µM
10 µM
c (propeptide)
D
rec. meprin β
relative meprin β activity
untreated
1 µM
5 µM
10 µM
50 µM
c (actinonin)
E
rec. meprin β
relative meprin β activity
untreated
50 nM
100 nM
300 nM
500 nM
c (fetuin-B)
F
(mca)-EDE
DED-(dnp)
(mca)-EDEDED-(dnp)
meprin β
ADAM10
shed meprin β
relative meprin β activity
mock
meprin β transfected
untreated
untreated
100 nM
200 nM
300 nM
500 nM
750 nM
1 µM
1,5 µM
2 µM
5 µM
10 µM
c (propeptide)
G
shed meprin β
mock
meprin β transfected
relative meprin β activity
***
untreated
untreated
1.5 µM propeptide
7.5 µM actinonin
200 nM fetuin-B
H
(mca)-EDE
DED-(dnp)
(mca)-EDEDED-(dnp)
meprin β
membrane-bound meprin β
relative meprin β activity
mock
meprin β transfected
untreated
untreated
100 nM
200 nM
300 nM
500 nM
750 nM
1 µM
1,5 µM
2 µM
5 µM
10 µM
c (propeptide)
I
membrane-bound meprin β
mock
meprin β transfected
relative meprin β activity
***
***
***
untreated
untreated
1.5 µM propeptide
7.5 µM actinonin
200 nM fetuin-B

Fig. 1 Meprin β is inhibited by its synthetic propeptide. (**A**) Protein structure models of pro-meprin β (left) compared to structure of the complex of propeptide (orange) added to active meprin β (generated with AlphaFold Server using the UniProt Consortium 2021 sequence and illustrated with ChimeraX1.9). In the sequence below, amino acids important for the interaction of the propeptide with Zn^{2+} and S1' position within the active site are highlighted. (**B**) Recombinant meprin β (30 nM) was fluorescence labeled and incubated with different concentrations of synthetically produced propeptide ranging from 6 pM to 50 µM. The dissociation constant (K_D) was calculated using the NanoTemper software. (**C**),(**D**),(**E**) Recombinant meprin β was preincubated with different concentrations of its synthetic propeptide, actinonin or fetuin-B. Meprin β activity was measured using a quenched fluorogenic peptide substrate ($n=3$). IC_{50} values were calculated. The propeptide is depicted in orange. (**F**), (**G**) HEK ADAM10/17$^{-/-}$ cells were transfected with meprin β and ADAM10. The conditioned supernatant was preincubated with different concentrations of its synthetic propeptide, actinonin or fetuin-B. Meprin β activity was measured using a quenched fluorogenic peptide substrate ($n=3$). The propeptide is depicted in orange. The significance in (**G**) was determined by one-way ANOVA with Bonferroni adjustment (ns: $p \geq 0.05$; ***: $p < 0.001$). (**H**),(**I**) HEK cells transfected with meprin β were preincubated with different concentrations of its synthetic propeptide, actinonin or fetuin-B. Meprin β activity at the cell surface was measured using a quenched fluorescent peptide substrate ($n=3$). The propeptide is depicted in orange. The significance in (**I**) was determined by one-way ANOVA with Bonferroni adjustment (***: $p < 0.001$)

The inhibitory capacity of the propeptide is increased by truncation of the C-terminus

In a targeted approach, we aimed to investigate how truncation of the termini influences the inhibitory capacity of the propeptide. Given the significance of D36 in its interaction with R238 and the crucial role of D49 in binding to the zinc ion within the active site cleft [13], we preserved these residues and their neighboring amino acids (Fig. 3A). Notably, we observed that truncating the C-terminus resulted in significant increase of the inhibitory capacity (Fig. 3B). Surprisingly, when the N-terminus was removed, no inhibitory capacity of this truncated propeptide could be observed anymore. As previously demonstrated in an experimentally solved crystal structure of pro-meprin β (PDB: 4GWM) [32] (Fig. 3C), the N-terminal part of the propeptide is in close proximity to both the catalytic and tumor necrosis factor receptor-associated factor (TRAF) domain of meprin β, harboring critical interaction sites for propeptide binding (Fig. 3C-G). In contrast, the C-terminal loop of the

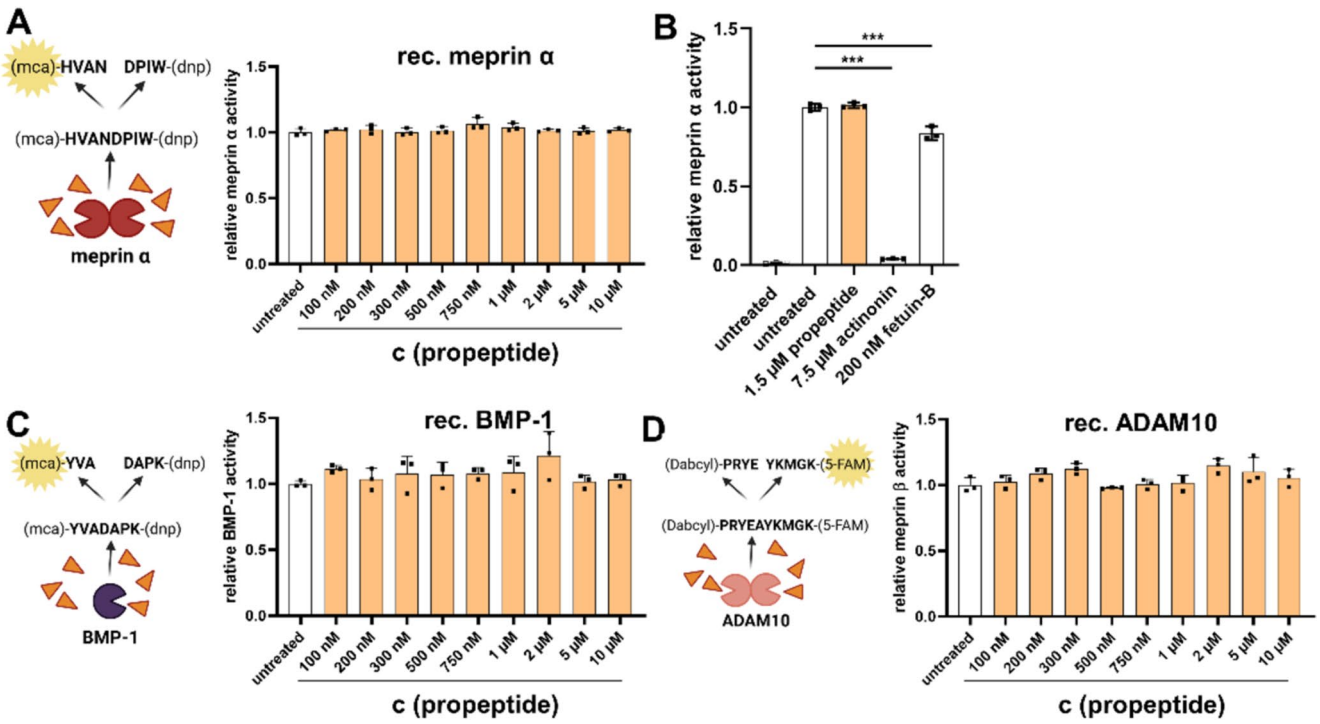

Fig. 2 The inhibitory capacity of the synthetic propeptide is specific for meprin β. (**A**), (**B**) Recombinant meprin α (5 nM), (**C**) recombinant BMP1 (5 nM) or (**D**) recombinant ADAM10 (5 nM) was preincubated with different concentrations of the synthetic propeptide of meprin β, actinonin or fetuin-B. The meprin α or BMP1 activity was measured using a quenched fluorescent peptide substrate ($n=3$). The propeptide is depicted in orange. The significance in (**B**) was determined by one-way ANOVA with Bonferroni adjustment (ns: $p \geq 0.05$; ***: $p < 0.001$)

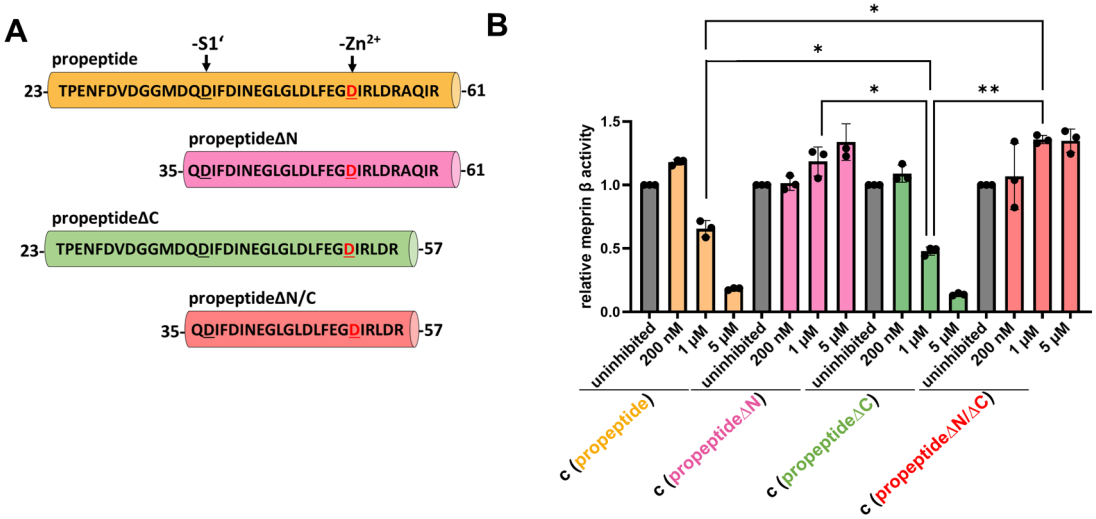

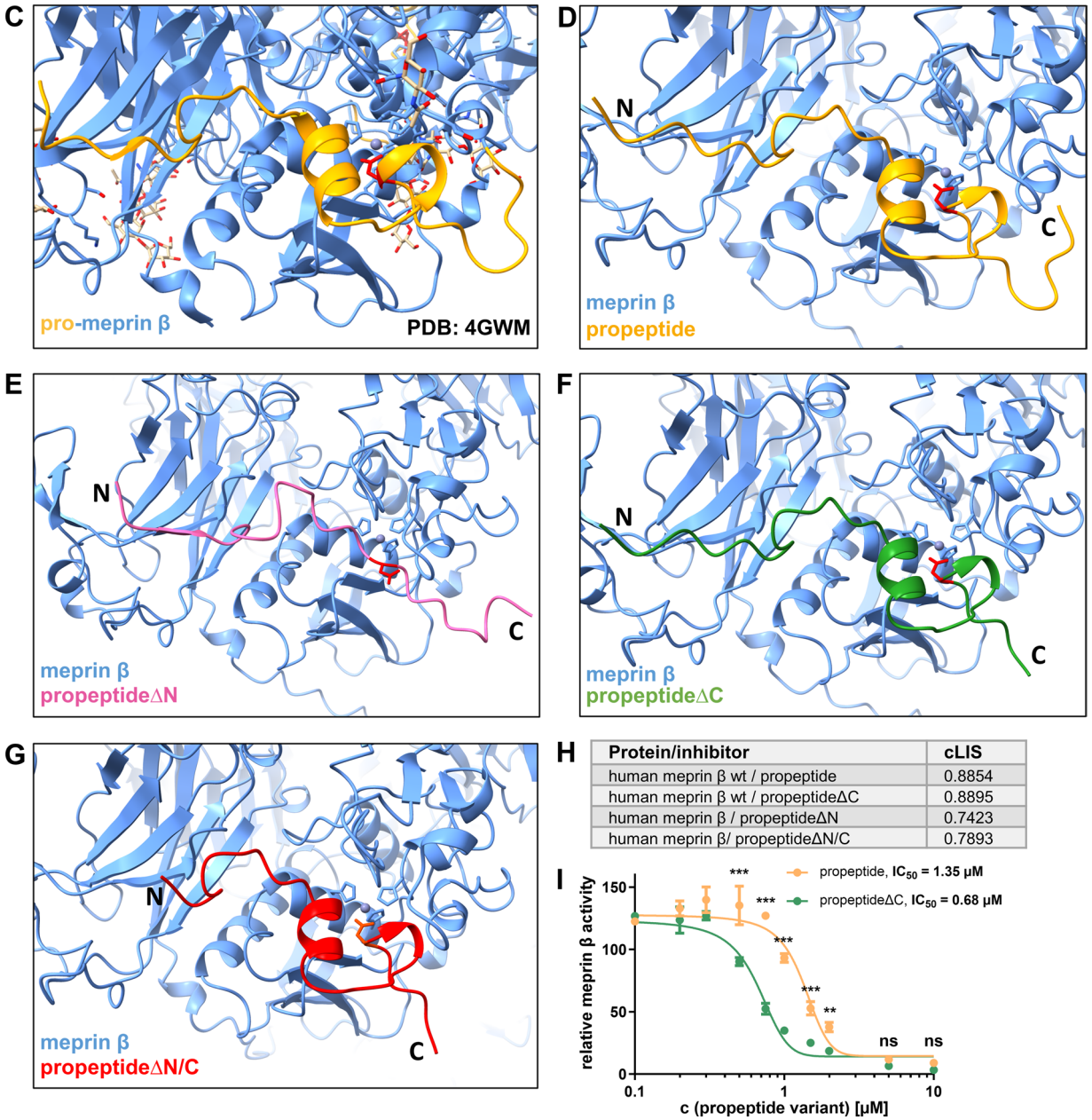

H

Protein/inhibitor	cLIS
human meprin β wt / propeptide	0.8854
human meprin β wt / propeptideΔC	0.8895
human meprin β / propeptideΔN	0.7423
human meprin β/ propeptideΔN/C	0.7893

Fig. 3 The inhibitory capacity of the propeptide is increased by truncation of the C-terminus. (A) Amino acid sequences of propeptide variants are depicted. D36, located on the bottom of the S1' site, and D52 (red), binding the zinc ion in the active site, are underlined. (B) Recombinant meprin β (5 nM) was preincubated with different concentrations of propeptide variants as depicted in (A). The meprin β activity was measured using a quenched fluorogenic peptide substrate (n = 3). The significance was determined by two-way ANOVA with Bonferroni adjustment (ns: $p \geq 0.05$; ***: $p < 0.001$). (C) Crystal structure of dimeric pro-meprin β (PDB: 4GWM)32 with close-up view on the propeptide. (D-G) Protein structure models of meprin β together with indicated propeptide variants from (A). Protein structures were generated with AlphaFold Server using the UniProt Consortium 2021 sequence (UniProt ID: Q16820) and visualized using ChimeraX1.9. (I) Local interaction score in contact interface (cLIS) of the interaction of meprin β together with different propeptide variants, calculated as described in 33. (H) Recombinant meprin β was preincubated with different concentrations of propeptide and propeptideΔC. Meprin β activity was measured using a quenched fluorogenic peptide substrate (n = 3). The significance was determined by two-way ANOVA with Bonferroni adjustment (ns: $p \geq 0.05$; **: $p < 0.001$; ***: $p < 0.001$)

propeptide protrudes away from the catalytic domain of meprin β. As a result, no crucial interaction sites are present in this region, and its deletion seems to confer a sterical advantage. Calculation of local interaction score in the contact interface (cLIS, normalized between 0 (very low confidence of interaction) and 1 (very high confidence of interaction) as described in [33]) further supports these findings, as cLIS was decreased for propeptide ΔN and propeptide ΔN/C compared to propeptide und propeptideΔC (Fig. 3H). Consequently, this led to a decrease in the IC_{50} from 1.35 µM for the wild-type propeptide to 0.68 µM for propeptideΔC (Fig. 3I).

To assess the specificity of propeptideΔC, we analyzed its potential inhibitory effects on a panel of other metalloproteases, including angiotensin-converting enzyme 1 (ACE1), ACE2, ADAM17, MMP1, MMP2, MMP14, and ovastacin (Supplementary Figure S3). No effect of propeptideΔC on the proteolytic activity of these metalloproteases was observed, with the exception of ovastacin, whose activity was significantly reduced at propeptideΔC concentrations of ≥1 µM.

The synthetic propeptide is a weak inhibitor of the cancer associated meprin β R238Q variant

We tested the inhibitory capacity of the propeptide towards the cancer-associated meprin β R238Q variant described in [13]. This variant was found in various cancer tissues and harbors a mutation in the S1' site of meprin β. R238, located at the bottom of this specificity pocket, predominantly governs the preference for acidic amino acids and interacts with D36 of the propeptide (Fig. 4A). With the substitution R238Q in meprin β, D36 of the propeptide lacks a partner for forming an ionic interaction, potentially leading to reduced inhibition upon exogenous addition of the propeptide. Indeed, in a peptide cleavage assay we observed that application of 1 µM of the propeptide resulted in inhibition of meprin β wt by 99%, while the variant meprin β R238Q is not inhibited at all (Fig. 4B). Only when the propeptide concentration was increased to 5 µM we observed inhibition of the meprin β R238Q variant of 70%. This outcome underscores how specificity is enabled by intermolecular interactions between meprin β and its propeptide, in particular involving the S1' position (Fig. 4C). To generate a propeptide inhibitor with improved efficacy against the cancer-associated meprin β R238Q variant, the aspartate at position 36 (D36) in the propeptide was replaced by a smaller alanine residue. Indeed, this leads to a more efficient inhibition of meprin β R238Q, while at the same time the inhibition of meprin β wt by propeptidΔC D36A was strongly reduced compared to propeptideΔC. This is reflected in the calculated K_i values obtained for the various combinations of meprin β and propeptide variants (Fig. 4G–J). Meprin β wt is efficiently inhibited by propeptideΔC, with a K_i of 0.019 µM, whereas the K_i value for inhibition of meprin β R238Q by propeptideΔC is markedly increased to 0.352 µM. The opposite effect is observed for the optimized propeptideΔC D36A variant: the K_i for propeptideΔC D36A for the meprin β R238Q with 0.092 µM is lower compared to 10.56 µM for meprin β wt, indicating substantially increased inhibitory potency against the cancer-associated variant.

Substrate cleavage by meprin β is inhibited by the synthetic propeptide *in cellulo*

To assess whether the propeptide variants also inhibit the cleavage of meprin β substrates in a cellular context, we transfected HEK cells with meprin β and the well-established meprin β substrates IL-6R [8], latrophilin-3 [35] as well as the amyloid precursor protein (APP)6. Transfecting HEK cells with meprin β and IL-6R, resulted in a 55 kDa cleavage fragment that accumulates in the supernatant (Fig. 5A, B). In the presence of the propeptide, the levels of the released IL-6R cleavage fragment are reduced in a concentration-dependent manner. This effect is even more pronounced when propeptideΔC was added.

Upon transfection of HEK cells with meprin β and latrophilin-3, the full-length form of latrophilin-3 in the lysate is decreased, and simultaneously, a 90 kDa cleavage fragment in the lysate and a 55 kDa fragment in the supernatant accumulates (Fig. 5C, D). In the presence of the propeptide, these proteolytic effects on latrophilin-3 were diminished in a concentration-dependent manner.

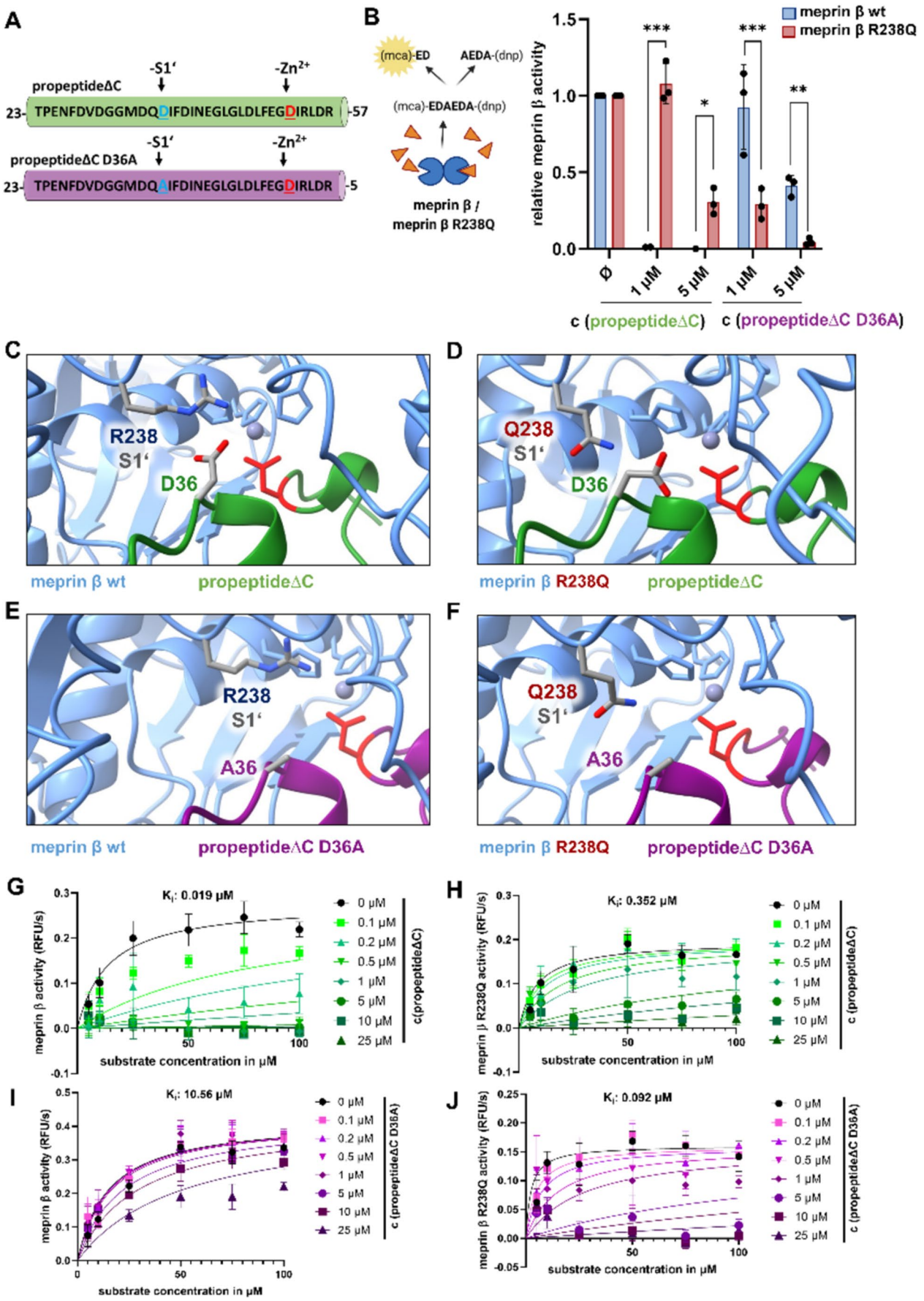
A
propeptideΔC
-S1'
-Zn2+
23- TPENFDVDGGMDQDIFDINEGLGLDLFEGDIRLDR -57
propeptideΔC D36A
-S1'
-Zn2+
23- TPENFDVDGGMDQAIFDINEGLGLDLFEGDIRLDR -5
B
(mca)-ED
AEDA-(dnp)
(mca)-EDAEDA-(dnp)
meprin β / meprin β R238Q
meprin β wt
meprin β R238Q
relative meprin β activity
1.5
1.0
0.5
0.0
***
***
*
**
Ø
1 µM
5 µM
1 µM
5 µM
c (propeptideΔC)
c (propeptideΔC D36A)
C
R238
S1'
D36
meprin β wt
propeptideΔC
D
Q238
S1'
D36
meprin β R238Q
propeptideΔC
E
R238
S1'
A36
meprin β wt
propeptideΔC D36A
F
Q238
S1'
A36
meprin β R238Q
propeptideΔC D36A
G
Ki: 0.019 µM
meprin β activity (RFU/s)
substrate concentration in µM
0 µM
0.1 µM
0.2 µM
0.5 µM
1 µM
5 µM
10 µM
25 µM
c(propeptideΔC)
H
Ki: 0.352 µM
meprin β R238Q activity (RFU/s)
substrate concentration in µM
c (propeptideΔC)
I
Ki: 10.56 µM
meprin β activity (RFU/s)
substrate concentration in µM
c (propeptideΔC D36A)
J
Ki: 0.092 µM
meprin β R238Q activity (RFU/s)
substrate concentration in µM
c (propeptideΔC D36A)

Fig. 4 Optimization of the propeptide for the inhibition of the cancer-associated variant meprin β R238Q. (**A**) Sequences of propeptide variants (propeptideΔC and propeptideΔC D36A) are depicted. For propeptideΔC D36A, the aspartate located on the bottom of the S1' site was replaced by an alanine residue for a better inhibition of the meprin β R238Q variant. (**B**) Recombinant wt meprin β (5 nM) and the R238Q variant were preincubated with the synthetically produced propeptideΔC and propeptideΔC D36A. The meprin β activity was measured using a quenched fluorogenic peptide substrate ($n=3$). The significance was determined by one-way ANOVA with Bonferroni adjustment (ns: $p \geq 0.05$; ***: $p < 0.001$). The propeptide is depicted in orange. (**C-F**) Protein structure models of meprin β wt and meprin β R238Q together with propeptideΔC and propeptideΔC D36A. Structures were generated with AlphaFold Server using the UniProt Consortium 2021 sequence and visualised using ChimeraX1.9. (**G-J**) Recombinant wt meprin β (5 nM) and the R238Q variant were preincubated with the synthetically produced propeptideΔC and propeptideΔC D36A in different concentrations. The meprin β activity was measured using different concentrations of a quenched fluorogenic peptide substrate ((mca)-EDAEDA-(dnp)) ($n=3$). To determine competitive inhibition enzyme activity across varying substrate and inhibitor concentrations were measured and K_i (inhibition constant) values were determined using GraphPad Prism [34]

Meprin β acts as an alternative β-secretase, generating pre-dominantly N-terminally truncated $Aβ_{2-x}$ peptides (Fig. 5E) 6, which are highly abundant in Alzheimer's disease (AD) patients' brains [36]. Co-transfection of meprin β and APP, compared to transfection with APP only, leads to higher amounts of sAPPβ (~100 kDa, detected with a neo-epitope specific antibody [22]) and a contrary effect on sAPPα fragments (~100 kDa), produced by α-secretases such as a ADAM10 or ADAM17 [37] (Fig. 5F). In the presence of the propeptide, and even more efficiently by the propeptideΔC, the generation of sAPPβ by meprin β was reduced in a concentration-dependent manner. Due to the competition of α-secretases and β-secretases for the processing of APP, successful inhibition of meprin β by the propeptide is also detectable by elevated sAPPα generation (Fig. 5F). Furthermore, an $Aβ_{x-40}$-ELISA showed a significant inhibitory effect of the propeptide inhibitors on generation of neurotoxic Aβ peptides (Fig. 5G).

Latrophilin-3 cleavage by meprin β is inhibited by the improved propeptideΔC in ex vivo cultivated brain slices

To determine whether inhibition of meprin β by propeptideΔC is effective in a more physiological context, we employed ex vivo cultivated brain slices. Given that the previously analyzed meprin β substrate latrophilin-3 is highly expressed in astrocytes, we utilized conditional knock-in mice that overexpress meprin β in astrocytes under the GFAP-promotor [23]. After generating the organotypic brain slices, they were cultivated and treated with propeptideΔC (Fig. 6A).

In brain lysates of the $GFAP^{Cre+/-}$;$Rosa26^{Mep1b-HA}$ mice overexpressing meprin β, the band corresponding to full-length latrophilin-3 at 130 kDa was decreased, whereas a cleavage fragment of 100 kDa was increased compared to control brain lysates. Treatment with propeptideΔC resulted in a reduction of the cleavage fragment (Fig. 6B). By quantifying the ratio between cleaved and full-length latrophilin-3, we observed a significant inhibition of meprin β-mediated latrophilin-3 cleavage by propeptideΔC (Fig. 6C). To evaluate the potential in vivo applicability of propeptideΔC as a therapeutic inhibitor, we assessed its stability under various pH and temperature conditions as well as its susceptibility to proteolytic degradation (Supplementary Figure S4). PropeptideΔC remained stable over a broad pH range (pH 1–10) and at temperatures up to 95 °C, and it also tolerated multiple freeze–thaw cycles without loss of inhibitory capacity. In contrast, pre-incubation with trypsin, and to a lesser extent with chymotrypsin or thrombin, reduced the inhibitory capacity of propeptideΔC, likely due to proteolytic processing of the inhibitor. Importantly, pre-incubation with murine serum did not affect the inhibitory capacity of propeptideΔC. Taken together, these results identified propeptideΔC as a highly stable and selective inhibitor with promising characteristics for future in vivo studies.

Discussion

Meprin β is an astacin metalloprotease that is upregulated in several pathological conditions [1]. For instance, elevated levels of meprin β have been detected in the brains of Alzheimer's disease patients, where it may contribute to the generation of neurotoxic Aβ peptides [6, 7]. In peripheral tissues such as skin and lung, meprin β participates in extracellular matrix remodeling and has been implicated in fibrotic processes, partly through cleavage of collagen and other matrix components [5, 8, 38]. In addition, meprin β modulates inflammatory responses through proteolytic processing of cytokines and cytokine receptors. It has been shown to activate pro-IL-1β and pro-IL-18 into their bioactive forms, thereby promoting inflammation [39]. Furthermore, meprin β can cleave the membrane-bound IL-6R, generating soluble IL-6R and enabling IL-6 trans-signaling [8]. Notably, meprins can also directly cleave and inactivate IL-6 itself, indicating a complex and context-dependent role in regulating IL-6–mediated signaling [8].To achieve a treatment with minimal side effects for pathologies associated with meprin β, the use of therapeutic inhibitors is a promising option. However, actinonin [9] and fetuin-B [12], the currently available inhibitors for meprin β, do not meet

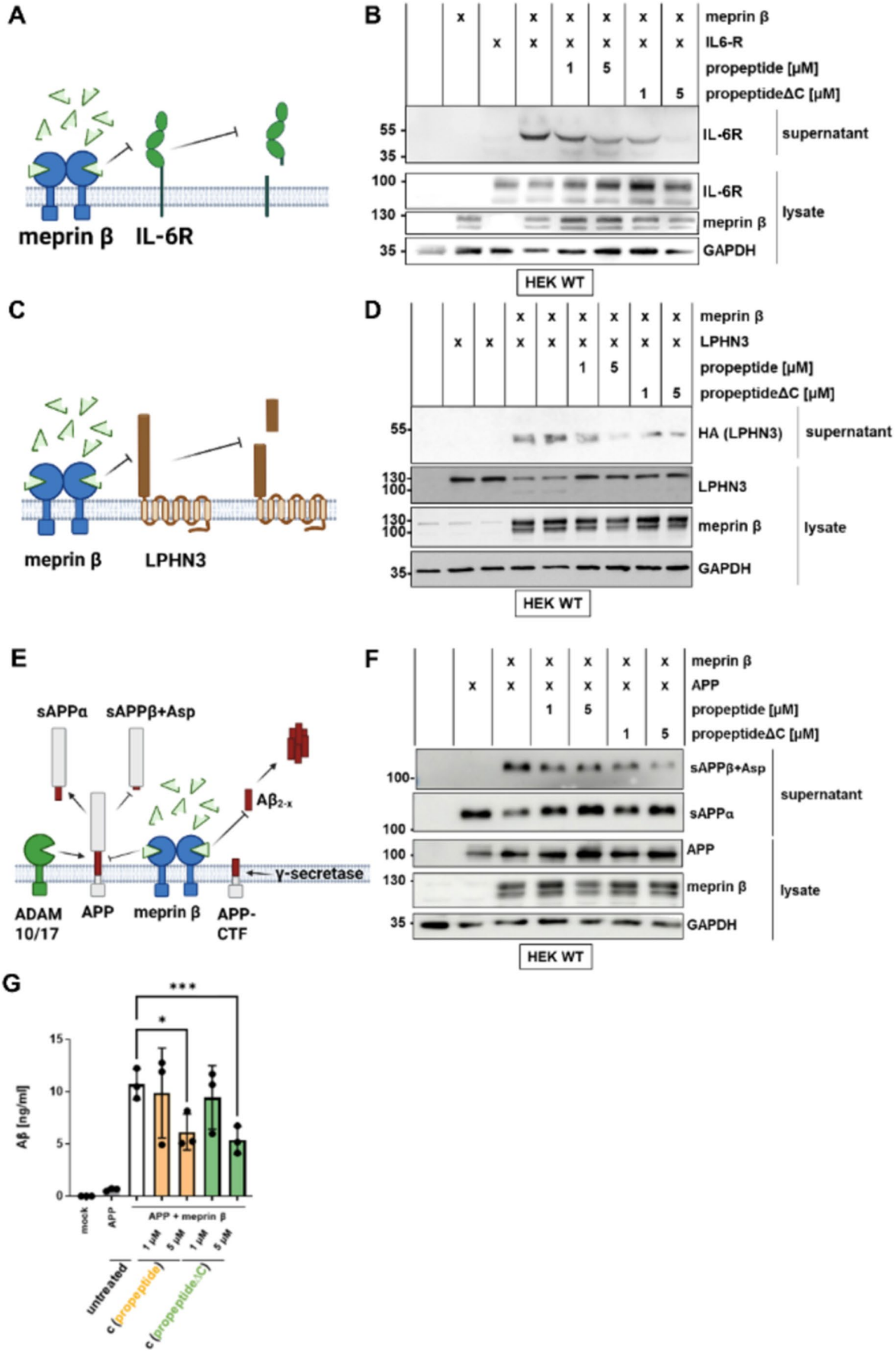
A
meprin β
IL-6R
B
meprin β
IL6-R
propeptide [µM]
propeptideΔC [µM]
55
35
IL-6R
supernatant
100
130
35
IL-6R
meprin β
GAPDH
lysate
HEK WT
C
meprin β
LPHN3
D
meprin β
LPHN3
propeptide [µM]
propeptideΔC [µM]
55
HA (LPHN3)
supernatant
130
100
LPHN3
130
100
meprin β
35
GAPDH
lysate
HEK WT
E
sAPPα
sAPPβ+Asp
Aβ2-x
γ-secretase
ADAM 10/17
APP
meprin β
APP-CTF
F
meprin β
APP
propeptide [µM]
propeptideΔC [µM]
100
sAPPβ+Asp
supernatant
100
sAPPα
100
APP
130
meprin β
lysate
35
GAPDH
HEK WT
G
Aβ [ng/ml]
15
10
5
0
***
*
mock
APP
APP + meprin β
1 µM
5 µM
1 µM
5 µM
untreated
c (propeptide)
c (propeptideΔC)

Fig. 5 Substrate cleavage by meprin β is inhibited by the synthetic propeptide in transfected HEK cells. (**A**) Scheme showing the propeptide inhibition of meprin β-mediated IL-6R cleavage. (**B**) HEK cells were transfected with IL-6R and/or meprin β. Afterwards, the cells were treated with the indicated concentration of propeptide or propeptideΔC. The cells were lysed and proteins were analyzed in cell lysates and supernatants using SDS-PAGE and Western blot ($n=3$). (**C**) Scheme showing the propeptide inhibition of meprin β-mediated latrophilin-3 cleavage. (**D**) HEK cells were transfected with latrophilin-3 and/or meprin β and analyzed as described in (B). (**E**) Scheme showing APP processing and propeptide inhibition of meprin β-mediated APP cleavage. (**F**) HEK cells were transfected with APP and/or meprin β and analyzed as described in (B). (**G**) $A\beta_{x-40}$-ELISA of supernatants from cells treated as described in (F). The significance was determined by two-way ANOVA with Bonferroni adjustment (ns: $p \geq 0.05$; **: $p < 0.001$; ***: $p < 0.001$)

the requirements in terms of specificity and, for fetuin-B, in terms of size and accessibility the of membrane-bound protease. In this regard, peptide-based inhibitors could represent a more promising approach. A published phosphinic peptide-based F2 inhibitor for meprin β [13] has been developed, but synthesis of this compound remains challenging and time-/cost-intensive. Furthermore, such phosphinic-based peptides are more likely to cause an immune response when applied in vivo. Thus, the use of endogenously occurring peptides may represent a preferable approach.

Therefore, in this study, we characterized the synthetically produced cognate meprin β propeptide as a competitive inhibitor for the enzyme. We demonstrated that the propeptide effectively inhibits both membrane-bound and soluble forms of meprin β with an inhibition constant in the micromolar range. Other meprin β-related proteases, such as meprin α and BMP-1 from the astacin family [40], as well as ADAM10, ADAM17, MMP1, MMP2 and MMP14 from the metzincin superfamily, are not inhibited by the propeptide, demonstrating the specificity of the compound for meprin β. Importantly, also activity of ACE1 and ACE2, which colocalize with meprin β in the kidney [41], is not affected by the cognate meprin β propeptide. However, we observed that the activity of the closely-related astacin protease ovastacin, is reduced by the addition of 1 µM or higher concentrations of the meprin β propeptide inhibitor. Ovastacin, like meprins exhibits a strong preference for aspartate in P1' position [42]. From our experiments, it remains unclear whether the observed effect results from the meprin β propeptide acting

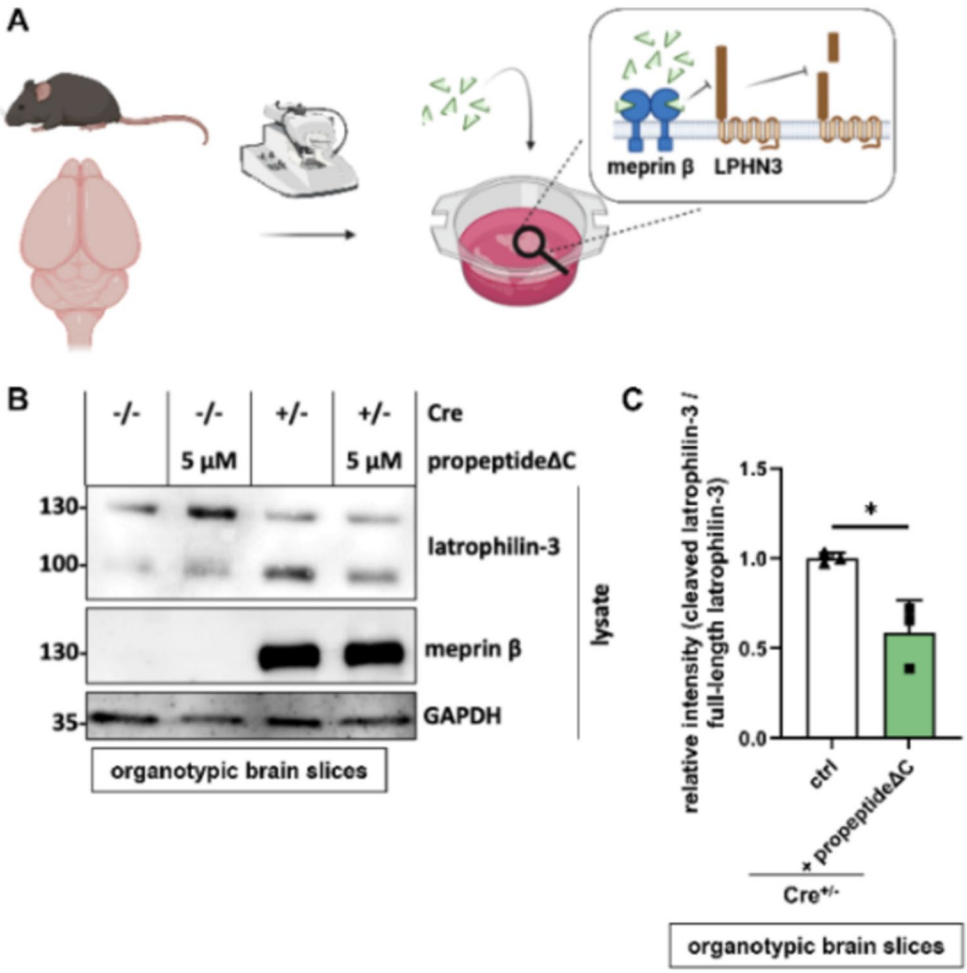

Fig. 6 Substrate cleavage by meprin β is inhibited by the improved propeptideΔC in *ex vivo* cultivated brain slices. (**A**) Organotypic brain slices were obtained by sagittal cutting the brain into 250 µm thick slices. Slices were cultivated for 20 days and treated with propeptideΔC (**B**) Organotypic brain slices of $GFAP^{Cre+/-}$;$Rosa26^{Mep1b-HA}$ and $GFAP^{Cre-/-}$;$Rosa26^{Mep1b-HA}$ mice. Half of the brain slices of each genotype were randomly selected and treated with 5 µM propeptideΔC, whereas the rest was left untreated. The organotypic brain slices were lysed and proteins were analyzed with SDS-PAGE and Western blot ($n=3$). (**C**) The Western blot signals for latrophilin-3 in panel (B) were quantified ($n=3$). The intensity of the signal corresponding to the 90 kDa cleavage fragment was measured relative to that of the full-length form at 130 kDa. The significance was determined by an unpaired t-test (*: $p < 0.05$)

as an inhibitor of ovastacin or as a competing substrate. However, given that ovastacin expression is restricted to oocytes, the observed effect is unlikely to have a significant impact on the potential therapeutic use of the inhibitor under pathophysiological conditions [40, 42, 43]. The observed specificity is a significant improvement over commonly used meprin β inhibitors. Typically, broad-spectrum metalloproteinase inhibitors like actinonin, galardin and batimastat are employed, whose mode of function is primarily based on zinc chelation through a hydroxamate group [9, 44–46]. Furthermore, TAPI-1, and TAPI-2, also inhibit meprin β activity [9]. However, several members of the metzincin family are targeted by these inhibitors, particularly matrix metalloproteinases (MMPs), which are affected to a much greater extent than meprin β. This makes these broad-spectrum inhibitors unsuitable for therapeutic applications that specifically target meprin β. More selective hydroxamate-based inhibitors have been developed, published lately in [47–49], showing inhibition in the in the lower nanomolar range, however, still facing problems typical for hydroxamates like metabolic instability, for example in plasma, and toxic metabolic byproducts [50].

Another prominent and endogenous inhibitor of meprin β is the plasma protein fetuin-B. Fetuin-B has been shown to inhibit meprin β in the nanomolar range [12]. However, the specificity is still an issue as it also inhibits closely related proteases like meprin α or ovastacin. Another drawback of fetuin-B is the molecular weight of 40 kDa, which would lead to high production costs of the recombinant protein or batch to batch variances. Furthermore, we observed that while soluble meprin β is strongly inhibited by fetuin-B, the potency is significantly reduced towards membrane-bound meprin β. As previously discussed, inhibition by fetuin-B probably requires a molecular rearrangement of the meprin β dimer from a "membrane-distal" to a "membrane-proximal" conformation [19]. Therefore, the propeptide has advantages over fetuin-B in terms of size, specificity, and accessibility. By deleting amino acids from the N- and C-termini of the synthetic meprin β propeptide, we observed that the N-terminus, which interacts with the TRAF and catalytic domain of meprin β, is crucial for appropriate binding of the propeptide. However, removing the C-terminal loop improves the inhibitory capacity and leads to increased inhibition of substrate cleavage, as demonstrated with the well-established substrates IL-6R, latrophilin-3 and APP. IL-6R serves as the receptor for the key regulatory cytokine IL-6. Shedding of IL-6R by meprin β enables a process known as IL-6 trans-signaling, where shed IL-6R binds to IL-6 and subsequently activates signaling via gp130 on cells that do not express IL-6R [8, 51]. Excessive trans-signaling may lead to detrimental pro-inflammatory signaling [52]. Besides latrophilin-3, expressed by astrocytes, plays a crucial role in synapse formation by interacting with neuronal proteins during synapse development. Impaired latrophilin-3 function has been associated with hyperactivity in mice and attention deficit hyperactivity disorder (ADHD) in humans. Finally, upregulation of meprin β in AD patients' brains [7] and its function as an alternative β-secretase by generating truncated Aβ peptides [6], suggest meprin β as a potential target in AD. As shown *in cellulo* for these substrates propeptide inhibitors could presents promising options for therapeutic intervention. To investigate the inhibitory effect of the propeptide in a more physiological context, we utilized ex vivo cultured brain slices overexpressing meprin β in astrocytes. By applying the propeptide to these cultures, we demonstrated inhibition of endogenously expressed latrophilin-3 and its cleavage by meprin β in this model. This supports the feasibility of using the propeptide in potential in vivo applications, a strategy which has already been successfully implemented for ADAM17. In a tumor mouse model, where ADAM17 is a key driver of metastasis, the prodomain of ADAM17 was intravenously injected and led to decreased metastasis [16]. As shown for the cancer-associated variant meprin β R238Q, the synthetic cognate propeptide inhibitor can easily be optimized to inhibit cancer associated protease variants by the simple exchange of certain amino acids, which may be of interest regarding a personalized anti-cancer-therapy. This might also be a suitable strategy to decrease the interaction of the meprin β propeptide with ovastacin. Overall, peptide-based inhibitors show potential for high target specificity and low off-target activity and can be easily synthesized and modified. However, some limitations of peptide drugs require further discussion, e.g. poor membrane permeability and limited in vivo stability. Despite these disadvantages, peptides have both high affinity and specificity for their biological targets, thereby reducing adverse effects and toxicity. Furthermore, peptides generally exhibit lower immunogenicity, are able to modulate protein–protein interactions and can be produced cost-effectively. Peptide-based inhibitors comprise several options for peptide modifications, that can enhance inhibitory properties and enhance stability [52, 53]. Regarding the use of the meprin β propeptide inhibitor for in vivo application it might be necessary to increase the stability and bioavailability. As demonstrated in this study, the propeptide exhibits limited proteolytic stability toward serine proteases such as trypsin, chymotrypsin, and thrombin; however, its stability may be enhanced by rationally designed amino acid substitutions. Notably, in our in vitro testing the propeptide inhibitor is stable against preincubation with mouse serum, which is important for the options of intravenous injections. This observed stability may result from limited proteolytic activity in the circulation due to endogenous protease inhibitors and supports a potential suitability of our inhibitor for a targeted in vivo applications, which however requires more detailed investigations.

In summary, we characterized and optimized the synthetic propeptide of meprin β as a competitive inhibitor with promising molecular properties in terms of size, specificity, and bioavailability. The translation to in vivo applications in preclinical mouse experiments and clinical trials will be part of future studies.

Abbreviations

5-fam	5-carboxyfluorescein
AD	Alzheimer's disease
ADAM	a disintegrin and metalloproteinase
ADHD	attention deficit hyperactivity disorder
ANOVA with Bonferroni adjustment	analysis of variance
APP	amyloid precursor protein
BMP1	bone morphogenetic protein 1
dabcyl	Acetyl-dArg(3)-dGlu(3)-hexaminoyl-K-4-((4-(Dimethylamino)phenyl)azo) benzoic
DMEM	Dulbecco's Modified Eagle Medium
DTT	dithiothreitol
FBS	fetal bovine serum
GAPDH	glyceraldehyde 3-phosphate dehydrogenase
GFAP	glial fibrally acidic protein
GPCR	G protein-coupled receptor
HEK293T_A10/17$^{-/-}$	HEK293T cells deficient for ADAM10 and ADAM17
IL-6R	interleukin-6 receptor
KD	dissociation constant
latrophilin-3	latrophilin-3
MAM	meprin/A5 protein/receptor protein tyrosine phosphatase μ
mca	7-methyloxycoumarin-4-yl
dnp	K-ε-dinitrophenyl
MST	microscale thermophoresis
OBSC	organotypic brain slice culture
PBS	phosphate-buffered saline
PEI	polyethyleneimine
propeptideΔC	C-terminally truncated propeptide
RFU	relative fluorescent unit
SDS	sodium dodecyl sulfate
SDS-PAGE	SDS-polyacrylamide gel electrophoresis
TBS	tris-buffered saline
TRAF	tumor necrosis factor receptor-associated factor

Supplementary Information The online version contains supplementary material available at https://doi.org/10.1007/s00018-026-06361-4 .

Acknowledgments The authors thank Britta Hansen and Victoria Schamborsky (Biochemical Institute, Kiel, Germany) for technical support. We thank Franka Scharfenberg for scientific advice. Fetuin-B was kindly provided by Walter Stöcker (Mainz, Germany). Simone Prömel (University of Düsseldorf, Germany) kindly provided the expression plasmid containing latrophilin-3.

Author contributions FA designed and performed experiments, analyzed data and wrote main parts of the manuscript. HB designed and carried out experiments, analyzed data, performed structural analyses and edited the manuscript. KB designed and conducted experiments, analyzed data, performed structural analyses and wrote and edited the manuscript. NS conducted experiments and analyzed data. SS, NA, NK and HK conducted experiments. CM and CUP supported the study with material and experiment design. IS and CBP conceived and supervised the project and edited the manuscript.

Funding This work was supported by the Deutsche Forschungsgemeinschaft (DFG) Project-numbers BE 535257441 GRK3085 (to CBP), 4086/9-1 (to CBP), 125440785 SFB 877 (Proteolysis as a Regulatory Event in Pathophysiology, Projects A9 (to CBP) and A15 (to CBP and CUP), a scholarship from the Jung Medal for Medicine in Gold 2023 (to KB, medal holder: Prof. Dr. Stefan Rose-John) and by the Alzheimer Forschung Initiative e.V. (AFI) project 18007 (to CBP and CUP).

Data availability Not applicable.

Declarations

Ethics approval All animal studies were conducted in compliance with European and German guidelines for the care and use of laboratory animals and were approved by the Central Animal Facility of the University of Kiel and the ethical committee on animal care and use of Schleswig-Holstein, Germany.

Competing interests and consent to publish The authors have no relevant financial or non-financial interests to disclose. All authors consented to publish the manuscript.

Open Access This article is licensed under a Creative Commons Attribution-NonCommercial-NoDerivatives 4.0 International License, which permits any non-commercial use, sharing, distribution and reproduction in any medium or format, as long as you give appropriate credit to the original author(s) and the source, provide a link to the Creative Commons licence, and indicate if you modified the licensed material. You do not have permission under this licence to share adapted material derived from this article or parts of it. The images or other third party material in this article are included in the article's Creative Commons licence, unless indicated otherwise in a credit line to the material. If material is not included in the article's Creative Commons licence and your intended use is not permitted by statutory regulation or exceeds the permitted use, you will need to obtain permission directly from the copyright holder. To view a copy of this licence, visit http://creativecommons.org/licenses/by-nc-nd/4.0/.

References

1. Broder C, Becker-Pauly C (2013) The metalloproteases meprin α and meprin β: unique enzymes in inflammation, neurodegeneration, cancer and fibrosis. Biochem J 450:253–264
2. Wichert R et al (2017) Mucus Detachment by Host Metalloprotease Meprin β Requires Shedding of Its Inactive Pro-form, which Is Abrogated by the Pathogenic Protease RgpB. Cell Rep 21:2090–2103
3. Bülck C et al (2023) Proteolytic processing of galectin-3 by meprin metalloproteases is crucial for host-microbiome homeostasis. Sci Adv 9:eadf4055
4. Werny L, Colmorgen C, Becker-Pauly C (2022) Regulation of meprin metalloproteases in mucosal homeostasis. Biochim et Biophys Acta (BBA) - Mol Cell Res 1869:119158
5. Broder C et al (2013) Metalloproteases meprin α and meprin β are C- and N-procollagen proteinases important for collagen assembly and tensile strength. Proc Natl Acad Sci U S A 110:14219–14224
6. Bien J et al (2012) The metalloprotease meprin β generates amino terminal-truncated amyloid β peptide species. J Biol Chem 287:33304–33313
7. Marengo L et al (2022) Meprin β knockout reduces brain Aβ levels and rescues learning and memory impairments in the APP/lon mouse model for Alzheimer's disease. Cell Mol Life Sci 79:168
8. Arnold P et al (2017) Meprin Metalloproteases Generate Biologically Active Soluble Interleukin-6 Receptor to Induce Trans-Signaling. Sci Rep 7:44053
9. Kruse M-N et al (2004) Human meprin alpha and beta homo-oligomers: cleavage of basement membrane proteins and sensitivity to metalloprotease inhibitors. Biochem J 378:383–389
10. Kousalová J et al (2022) Metastatic spread inhibition of cancer cells through stimuli-sensitive HPMA copolymer-bound actinonin nanomedicines. Nanomed Nanotechnol Biol Med 44:102578
11. Botos I, Scapozza L, Zhang D, Liotta LA, Meyer EF (1996) Batimastat, a potent matrix mealloproteinase inhibitor, exhibits an unexpected mode of binding. Proc Natl Acad Sci U S A 93:2749–2754
12. Karmilin K et al (2019) Mammalian plasma fetuin-B is a selective inhibitor of ovastacin and meprin metalloproteinases. Sci Rep 9:546
13. Bickenbach K et al (2025) Targeted approach to determine the impact of cancer-associated protease variants. Sci Adv 11:eadp5958
14. Moss ML et al (2007) The ADAM10 Prodomain Is a Specific Inhibitor of ADAM10 Proteolytic Activity and Inhibits Cellular Shedding Events. J Biol Chem 282:35712–35721
15. Wong E et al (2016) Harnessing the natural inhibitory domain to control TNFα Converting Enzyme (TACE) activity in vivo. Sci Rep 6:35598
16. Bolik J et al (2022) Inhibition of ADAM17 impairs endothelial cell necroptosis and blocks metastasis. J Exp Med 219:e20201039
17. Becker-Pauly C et al (2007) The α and β Subunits of the Metalloprotease Meprin Are Expressed in Separate Layers of Human Epidermis, Revealing Different Functions in Keratinocyte Proliferation and Differentiation. J Invest Dermatology 127:1115–1125
18. Blanc G et al (2007) Insights into How CUB Domains Can Exert Specific Functions while Sharing a Common Fold. J Biol Chem 282:16924–16933
19. Eckhard U, Körschgen H, Von Wiegen N, Stöcker W, Gomis-Rüth FX (2021) The crystal structure of a 250-kDa heterotetrameric particle explains inhibition of sheddase meprin β by endogenous fetuin-B. Proc Natl Acad Sci USA 118:e2023839118
20. Jerabek-Willemsen M et al (2014) MicroScale Thermophoresis: Interaction analysis and beyond. J Mol Struct 1077:101–113
21. Riethmueller S et al (2016) Cleavage Site Localization Differentially Controls Interleukin-6 Receptor Proteolysis by ADAM10 and ADAM17. Sci Rep 6:25550
22. Armbrust F et al (2024) A novel mouse model for N-terminal truncated Aβ2-x generation through meprin β overexpression in astrocytes. Cell Mol Life Sci 81:139
23. Scharfenberg F et al (2020) Degradome of soluble ADAM10 and ADAM17 metalloproteases. Cell Mol Life Sci 77:331–350
24. Talantikite M et al (2018) Inhibitors of BMP -1/tolloid-like proteinases: efficacy, selectivity and cellular toxicity. FEBS Open Bio 8:2011–2021
25. Werny L et al (2023) MT1-MMP and ADAM10/17 exhibit a remarkable overlap of shedding properties. FEBS J 290:93–111
26. Lu J, Sun PD (2020) High affinity binding of SARS-CoV-2 spike protein enhances ACE2 carboxypeptidase activity. Preprint at. https://doi.org/10.1101/2020.07.01.182659
27. Sriramula S, Pedersen KB, Xia H, Lazartigues E (2017) Determining the Enzymatic Activity of Angiotensin-Converting Enzyme 2 (ACE2) in Brain Tissue and Cerebrospinal Fluid Using a Quenched Fluorescent Substrate. Methods Mol Biol 1527:117–126
28. Jin G et al (2002) A continuous fluorimetric assay for tumor necrosis factor-alpha converting enzyme. Anal Biochem 302:269–275
29. Körschgen H et al (2020) A Primary Evaluation of Potential Small-Molecule Inhibitors of the Astacin Metalloproteinase Ovastacin, a Novel Drug Target in Female Infertility Treatment. ChemMedChem 15:1499–1504
30. Kuske M et al (2021) Limited proteolysis by acrosin affects sperm-binding and mechanical resilience of the mouse zona pellucida. Mol Hum Reprod 27:gaab022
31. Bertenshaw GP et al (2001) Marked Differences between Metalloproteases Meprin A and B in Substrate and Peptide Bond Specificity. J Biol Chem 276:13248–13255
32. Arolas JL et al (2012) Structural basis for the sheddase function of human meprin β metalloproteinase at the plasma membrane. Proc Natl Acad Sci USA 109:16131–16136
33. Kim A-R et al (2024) Enhanced protein-protein interaction discovery via alphafold-multimer 2024.02.19.58097. Preprint at https://doi.org/10.1101/2024.02.19.580970
34. Copeland RA (2005) Evaluation of enzyme inhibitors in drug discovery. A guide for medicinal chemists and pharmacologists. Methods Biochem Anal 46:1–265
35. Armbrust F et al (2025) HYTANE-Identified Latrophilin-3 Cleavage by Meprin β Leads to Loss of the Interaction Domains. J Proteome Res 24:1832–1844
36. Wiltfang J et al (2001) Elevation of β-Amyloid Peptide 2–42 in Sporadic and Familial Alzheimer's Disease and Its Generation in PS1 Knockout Cells. J Biol Chem 276:42645–42657
37. Asai M et al (2003) Putative function of ADAM9, ADAM10, and ADAM17 as APP alpha-secretase. Biochem Biophys Res Commun 301:231–235
38. Biasin V et al (2017) Meprin β contributes to collagen deposition in lung fibrosis. Sci Rep 7:39969
39. Banerjee S, Bond JS (2008) Prointerleukin-18 Is Activated by Meprin β in Vitro and in Vivo in Intestinal Inflammation. J Biol Chem 283:31371–31377
40. Gomis-Rüth FX, Stöcker W (2022) Structural and evolutionary insights into astacin metallopeptidases. Front Mol Biosci 9:1080836
41. Mathew R et al (2005) Meprin-α in chronic diabetic nephropathy: interaction with the renin-angiotensin axis. Am J Physiology-Renal Physiol 289:F911–F921
42. Felten M et al (2024) Substrate profiling of the metalloproteinase ovastacin uncovers specific enzyme–substrate interactions and discloses fertilization-relevant substrates. FEBS J 291:114–131

43. Burkart AD, Xiong B, Baibakov B, Jiménez-Movilla M, Dean J (2012) Ovastacin, a cortical granule protease, cleaves ZP2 in the zona pellucida to prevent polyspermy. J Cell Biol 197:37–44
44. Chen DZ et al (2000) Actinonin, a Naturally Occurring Antibacterial Agent, Is a Potent Deformylase Inhibitor. Biochemistry 39:1256–1262
45. Wojtowicz-Praga SM, Dickson RB, Hawkins MJ (1997) Matrix metalloproteinase inhibitors. Invest New Drugs 15:61–75
46. Tan K et al (2023) Synthesis and structure–activity relationships of pyrazole-based inhibitors of meprin α and β. J Enzyme Inhib Med Chem 38:2165648
47. Linnert M et al (2021) Structure and Dynamics of Meprin β in Complex with a Hydroxamate-Based Inhibitor. Int J Mol Sci 22:5651
48. Ramsbeck D et al (2018) Structure-Guided Design, Synthesis, and Characterization of Next-Generation Meprin β Inhibitors. J Med Chem 61:4578–4592
49. Ramsbeck D, Hamann A, Schlenzig D, Schilling S, Buchholz M (2017) First insight into structure-activity relationships of selective meprin β inhibitors. Bioorg Med Chem Lett 27:2428–2431
50. Fields GB (2019) The Rebirth of Matrix Metalloproteinase Inhibitors: Moving Beyond the Dogma. Cells 8:984
51. Rose-John S (2012) IL-6 Trans-Signaling via the Soluble IL-6 Receptor: Importance for the Pro-Inflammatory Activities of IL-6. Int J Biol Sci 8:1237–1247
52. Lau JL, Dunn MK (2018) Therapeutic peptides: Historical perspectives, current development trends, and future directions. Bioorg Med Chem 26:2700–2707
53. Wang L et al (2022) Therapeutic peptides: current applications and future directions. Sig Transduct Target Ther 7:48

Publisher's Note Springer Nature remains neutral with regard to jurisdictional claims in published maps and institutional affiliations.